

EUROPEAN ORGANIZATION FOR NUCLEAR RESEARCH

CERN-PH-EP/2006-003
3rd March 2006

QCD coherence and correlations of particles with restricted momenta in hadronic Z decays

The OPAL Collaboration

Abstract

QCD coherence effects are studied based on measurements of correlations of particles with either restricted transverse momenta, $p_T < p_T^{\text{cut}}$, where p_T is defined with respect to the thrust axis, or restricted absolute momenta, $p \equiv |\mathbf{p}| < p^{\text{cut}}$, using about four million hadronic Z decays recorded at LEP with the OPAL detector. The correlations are analyzed in terms of normalized factorial and cumulant moments. The analysis is inspired by analytical QCD calculations which, in conjunction with Local Parton-Hadron Duality (LPHD), predict that, due to colour coherence, the multiplicity distribution of particles with restricted transverse momenta should become Poissonian as p_T^{cut} decreases. The expected correlation pattern is indeed observed down to $p_T^{\text{cut}} \approx 1$ GeV but not at lower transverse momenta. Furthermore, for $p^{\text{cut}} \rightarrow 0$ GeV a strong rise is observed in the data, in disagreement with theoretical expectation. The Monte Carlo models reproduce well the measurements at large p_T^{cut} and p^{cut} but underestimate their magnitudes at the lowest momenta. The e^+e^- data are also compared to the measurements in deep-inelastic e^+p collisions. Our study indicates difficulties with the LPHD hypothesis when applied to many-particle inclusive observables of soft hadrons.

Submitted to Physics Letters B

The OPAL Collaboration

G. Abbiendi², C. Ainsley⁵, P.F. Åkesson^{3,y}, G. Alexander²¹, G. Anagnostou¹,
 K.J. Anderson⁸, S. Asai²², D. Axen²⁶, I. Bailey²⁵, E. Barberio^{7,p}, T. Barillari³¹,
 R.J. Barlow¹⁵, R.J. Batley⁵, P. Bechtel²⁴, T. Behnke²⁴, K.W. Bell¹⁹, P.J. Bell¹, G. Bella²¹,
 A. Bellerive⁶, G. Benelli⁴, S. Bethke³¹, O. Biebel³⁰, O. Boeriu⁹, P. Bock¹⁰,
 M. Boutemour³⁰, S. Braibant², R.M. Brown¹⁹, H.J. Burckhart⁷, S. Campana⁴,
 P. Capiluppi², R.K. Carnegie⁶, A.A. Carter¹², J.R. Carter⁵, C.Y. Chang¹⁶,
 D.G. Charlton¹, C. Ciocca², A. Csilling²⁸, M. Cuffiani², S. Dado²⁰, A. De Roeck⁷, E.A. De
 Wolf^{7,s}, K. Desch²⁴, B. Dienes²⁹, J. Dubbert³⁰, E. Duchovni²³, G. Duckeck³⁰,
 I.P. Duerdoth¹⁵, E. Etzion²¹, F. Fabbri², P. Ferrari⁷, F. Fiedler³⁰, I. Fleck⁹, M. Ford¹⁵,
 A. Frey⁷, P. Gagnon¹¹, J.W. Gary⁴, C. Geich-Gimbel³, G. Giacomelli², P. Giacomelli²,
 M. Giunta⁴, J. Goldberg²⁰, E. Gross²³, J. Grunhaus²¹, M. Gruwé⁷, P.O. Günther³,
 A. Gupta⁸, C. Hajdu²⁸, M. Hamann²⁴, G.G. Hanson⁴, A. Harel²⁰, M. Hauschild⁷,
 C.M. Hawkes¹, R. Hawkings⁷, G. Herten⁹, R.D. Heuer²⁴, J.C. Hill⁵, D. Horváth^{28,c},
 P. Igo-Kemenes¹⁰, K. Ishii²², H. Jeremie¹⁷, P. Jovanovic¹, T.R. Junk^{6,i}, J. Kanzaki^{22,u},
 D. Karlen²⁵, K. Kawagoe²², T. Kawamoto²², R.K. Keeler²⁵, R.G. Kellogg¹⁶,
 B.W. Kennedy¹⁹, S. Kluth³¹, T. Kobayashi²², M. Kobel³, S. Komamiya²², T. Krämer²⁴,
 A. Krasznahorkay Jr.^{29,e}, P. Krieger^{6,l}, J. von Krogh¹⁰, T. Kuhl²⁴, M. Kupper²³,
 G.D. Lafferty¹⁵, H. Landsman²⁰, D. Lanske¹³, D. Lellouch²³, J. Letts^o, L. Levinson²³,
 J. Lillich⁹, S.L. Lloyd¹², F.K. Loebinger¹⁵, J. Lu^{26,w}, A. Ludwig³, J. Ludwig⁹, W. Mader^{3,t},
 S. Marcellini², A.J. Martin¹², T. Mashimo²², P. Mättig^m, J. McKenna²⁶,
 R.A. McPherson²⁵, F. Meijers⁷, W. Menges²⁴, F.S. Merritt⁸, H. Mes^{6,a}, N. Meyer²⁴,
 A. Michelini², S. Mihara²², G. Mikenberg²³, D.J. Miller¹⁴, W. Mohr⁹, T. Mori²²,
 A. Mutter⁹, K. Nagai¹², I. Nakamura^{22,v}, H. Nanjo²², H.A. Neal³², R. Nisius³¹,
 S.W. O’Neale^{1,*}, A. Oh⁷, M.J. Oreglia⁸, S. Orito^{22,*}, C. Pahl³¹, G. Pásztor^{4,g}, J.R. Pater¹⁵,
 J.E. Pilcher⁸, J. Pinfold²⁷, D.E. Plane⁷, O. Pooth¹³, M. Przybycień^{7,n}, A. Quadt³,
 K. Rabbertz^{7,r}, C. Rembser⁷, P. Renkel²³, J.M. Roney²⁵, A.M. Rossi², Y. Rozen²⁰,
 K. Runge⁹, K. Sachs⁶, T. Saeki²², E.K.G. Sarkisyan^{7,j}, A.D. Schaile³⁰, O. Schaile³⁰,
 P. Scharff-Hansen⁷, J. Schieck³¹, T. Schörner-Sadenius^{7,z}, M. Schröder⁷, M. Schumacher³,
 R. Seuster^{13,f}, T.G. Shears^{7,h}, B.C. Shen⁴, P. Sherwood¹⁴, A. Skuja¹⁶, A.M. Smith⁷,
 R. Sobie²⁵, S. Söldner-Rembold¹⁵, F. Spano^{8,y}, A. Stahl^{3,x}, D. Strom¹⁸, R. Ströhmer³⁰,
 S. Tarem²⁰, M. Tasevsky^{7,d}, R. Teuscher⁸, M.A. Thomson⁵, E. Torrence¹⁸, D. Toya²²,
 P. Tran⁴, I. Trigger⁷, Z. Trócsányi^{29,e}, E. Tsur²¹, M.F. Turner-Watson¹, I. Ueda²²,
 B. Ujvári^{29,e}, C.F. Vollmer³⁰, P. Vannerem⁹, R. Vértési^{29,e}, M. Verzocchi¹⁶, H. Voss^{7,q},
 J. Vossebeld^{7,h}, C.P. Ward⁵, D.R. Ward⁵, P.M. Watkins¹, A.T. Watson¹, N.K. Watson¹,
 P.S. Wells⁷, T. Wengler⁷, N. Wormes³, G.W. Wilson^{15,k}, J.A. Wilson¹, G. Wolf²³,
 T.R. Wyatt¹⁵, S. Yamashita²², D. Zer-Zion⁴, L. Zivkovic²⁰

¹School of Physics and Astronomy, University of Birmingham, Birmingham B15 2TT, UK

²Dipartimento di Fisica dell’ Università di Bologna and INFN, I-40126 Bologna, Italy

- ³Physikalisches Institut, Universität Bonn, D-53115 Bonn, Germany
- ⁴Department of Physics, University of California, Riverside CA 92521, USA
- ⁵Cavendish Laboratory, Cambridge CB3 0HE, UK
- ⁶Ottawa-Carleton Institute for Physics, Department of Physics, Carleton University, Ottawa, Ontario K1S 5B6, Canada
- ⁷CERN, European Organisation for Nuclear Research, CH-1211 Geneva 23, Switzerland
- ⁸Enrico Fermi Institute and Department of Physics, University of Chicago, Chicago IL 60637, USA
- ⁹Fakultät für Physik, Albert-Ludwigs-Universität Freiburg, D-79104 Freiburg, Germany
- ¹⁰Physikalisches Institut, Universität Heidelberg, D-69120 Heidelberg, Germany
- ¹¹Indiana University, Department of Physics, Bloomington IN 47405, USA
- ¹²Queen Mary and Westfield College, University of London, London E1 4NS, UK
- ¹³Technische Hochschule Aachen, III Physikalisches Institut, Sommerfeldstrasse 26-28, D-52056 Aachen, Germany
- ¹⁴University College London, London WC1E 6BT, UK
- ¹⁵Department of Physics, Schuster Laboratory, The University, Manchester M13 9PL, UK
- ¹⁶Department of Physics, University of Maryland, College Park, MD 20742, USA
- ¹⁷Laboratoire de Physique Nucléaire, Université de Montréal, Montréal, Québec H3C 3J7, Canada
- ¹⁸University of Oregon, Department of Physics, Eugene OR 97403, USA
- ¹⁹CCLRC Rutherford Appleton Laboratory, Chilton, Didcot, Oxfordshire OX11 0QX, UK
- ²⁰Department of Physics, Technion-Israel Institute of Technology, Haifa 32000, Israel
- ²¹Department of Physics and Astronomy, Tel Aviv University, Tel Aviv 69978, Israel
- ²²International Centre for Elementary Particle Physics and Department of Physics, University of Tokyo, Tokyo 113-0033, and Kobe University, Kobe 657-8501, Japan
- ²³Particle Physics Department, Weizmann Institute of Science, Rehovot 76100, Israel
- ²⁴Universität Hamburg/DESY, Institut für Experimentalphysik, Notkestrasse 85, D-22607 Hamburg, Germany
- ²⁵University of Victoria, Department of Physics, P O Box 3055, Victoria BC V8W 3P6, Canada
- ²⁶University of British Columbia, Department of Physics, Vancouver BC V6T 1Z1, Canada
- ²⁷University of Alberta, Department of Physics, Edmonton AB T6G 2J1, Canada
- ²⁸Research Institute for Particle and Nuclear Physics, H-1525 Budapest, P O Box 49, Hungary
- ²⁹Institute of Nuclear Research, H-4001 Debrecen, P O Box 51, Hungary
- ³⁰Ludwig-Maximilians-Universität München, Sektion Physik, Am Coulombwall 1, D-85748 Garching, Germany
- ³¹Max-Planck-Institute für Physik, Föhringer Ring 6, D-80805 München, Germany
- ³²Yale University, Department of Physics, New Haven, CT 06520, USA

^a and at TRIUMF, Vancouver, Canada V6T 2A3

- ^c and Institute of Nuclear Research, Debrecen, Hungary
- ^d now at Institute of Physics, Academy of Sciences of the Czech Republic, 18221 Prague, Czech Republic
- ^e and Department of Experimental Physics, University of Debrecen, Hungary
- ^f and MPI München
- ^g and Research Institute for Particle and Nuclear Physics, Budapest, Hungary
- ^h now at University of Liverpool, Dept of Physics, Liverpool L69 3BX, U.K.
- ⁱ now at Dept. Physics, University of Illinois at Urbana-Champaign, U.S.A.
- ^j and Manchester University Manchester, M13 9PL, United Kingdom
- ^k now at University of Kansas, Dept of Physics and Astronomy, Lawrence, KS 66045, U.S.A.
- ^l now at University of Toronto, Dept of Physics, Toronto, Canada
- ^m current address Bergische Universität, Wuppertal, Germany
- ⁿ now at University of Mining and Metallurgy, Cracow, Poland
- ^o now at University of California, San Diego, U.S.A.
- ^p now at The University of Melbourne, Victoria, Australia
- ^q now at IPHE Université de Lausanne, CH-1015 Lausanne, Switzerland
- ^r now at IEKP Universität Karlsruhe, Germany
- ^s now at University of Antwerpen, Physics Department, B-2610 Antwerpen, Belgium; supported by Interuniversity Attraction Poles Programme – Belgian Science Policy
- ^t now at Technische Universität, Dresden, Germany
- ^u and High Energy Accelerator Research Organisation (KEK), Tsukuba, Ibaraki, Japan
- ^v now at University of Pennsylvania, Philadelphia, Pennsylvania, USA
- ^w now at TRIUMF, Vancouver, Canada
- ^x now at DESY Zeuthen
- ^y now at CERN
- ^z now at DESY
- * Deceased

1 Introduction

At high energies, the annihilation process $e^+e^- \rightarrow \text{hadrons}$ proceeds through the creation of a highly virtual primary quark and anti-quark which initiate a cascade of partons through successive parton emissions. The evolution of such a parton cascade is well understood in perturbative Quantum Chromodynamics (QCD) for virtualities, Q^2 , of the daughter partons larger than Q_0^2 . Here Q_0 is a virtuality cut-off below which the strong coupling constant becomes large and perturbative methods cease to be valid. In comparisons to experimental data, Q_0 was found to be of the order of hadronic masses ($Q_0 \sim \text{few hundred MeV}$).

A fundamental property of a QCD cascade, which follows from the non-Abelian structure of QCD, is colour coherence. This induces an angular ordering of subsequent emissions in the branching process [1] which restricts the phase space for each subsequent parton in the cascade. Angular ordering has important consequences of which we mention only a few (see [2–5] for a comprehensive review). Compared to a cascade without angular ordering, the single-parton inclusive distribution is suppressed for soft, or low-momentum, particles (the “hump-back” plateau) [6], the mean parton multiplicity evolves less rapidly with increasing jet energy, and the rapidity distribution becomes flat and energy independent for partons with very small transverse momenta [3].

It is remarkable that inclusive characteristics of *hadrons* measured in a variety of hard processes indeed show a behaviour similar to that expected from perturbative parton-level calculations [3–5]. This indicates that perturbative QCD effects and colour coherence in particular leave their imprint on the hadronic final state even for quantities which are not infra-red safe, such as particle multiplicity. The hypothesis of Local Parton-Hadron Duality (LPHD) [6] embodies these observations. According to LPHD, parton-level QCD predictions are applicable to sufficiently inclusive hadronic observables without the need for a hadronisation phase: hadronic spectra are proportional to those of partons if the cut-off Q_0 is decreased towards a small value of the order of Λ , the QCD-scale.

Within the LPHD picture, perturbative QCD calculations have been carried out in the Double Leading Logarithmic Approximation (DLA) or in the Modified Leading Logarithmic Approximation (MLLA) which includes terms of order $\sqrt{\alpha_s}$ in the strong coupling constant [2, 3]. The DLA calculations neglect energy-momentum conservation in gluon splittings which is partly taken into account in the MLLA. Although analytical calculations provide much valuable physical insight, they have often to be considered as qualitative. More quantitative results are obtained from parton-shower Monte Carlo models, the physics implementation of which strongly resembles the analytical calculations, but which impose energy-momentum conservation and include the complete parton-splitting functions.

In spite of its success with single-particle inclusive spectra, earlier studies have shown that the applicability of LPHD is less evident for the moments of single-particle densities at HERA energies [7] and angular correlations at LEP [8] and at HERA [9]. It is therefore of considerable importance to further test multiparticle aspects of perturbative QCD predictions, which are sensitive to colour coherence, in conjunction with LPHD.

Sensitive studies of colour coherence were suggested in [10] within DLLA calculations and using factorial moment and cumulant techniques. In a QCD cascade the presence of one gluon enhances the probability for further gluon emissions, causing positive correlations. The multiplicity distribution of partons in a jet is therefore generally broader than a Poisson distribution (which corresponds to uncorrelated production) and obeys asymptotic KNO-scaling [11]. However, it was pointed out in [10] that, due to colour coherence, gluons produced with bounded transverse momenta, $p_T < p_T^{\text{cut}}$, where p_T is defined with respect to the primary parton in a jet, become, for small p_T^{cut} , independently emitted from the primary parton. This implies that their multiplicity distribution becomes Poissonian, analogous to that of soft photons radiated from a charged particle in QED. In contrast, for gluons with bounded absolute momenta, $p \equiv |\mathbf{p}| < p^{\text{cut}}$, for which the angular ordering constraint is less important, the distribution remains non-Poissonian even for very small p^{cut} .

The DLLA analytical predictions were first tested in deep-inelastic e^+p scattering by the ZEUS experiment at HERA [12] using a sample of $\simeq 7500$ high- Q^2 events. Because of low statistics, factorial cumulants were not studied. The factorial moments were measured in the current region of the Breit frame [13]. From the significant discrepancies between data and both the DLLA calculations and parton-level ARIADNE Monte Carlo [14] expectations, the authors conclude that the LPHD hypothesis is strongly violated for many-particle observables. Monte Carlo models, which include hadronisation effects, reproduce the correlation pattern of the hadronic final state, although sizeable discrepancies remain for small values of p_T^{cut} and p^{cut} .

In this paper, we report the first results in e^+e^- annihilation on factorial moments and cumulants for hadrons with restricted transverse and absolute momenta in a jet. The measurements are based on a data sample of about four million Z hadronic decays recorded with the OPAL detector at the LEP e^+e^- collider at CERN.

2 Analysis

The calculations in [10] use factorial moments and cumulants known to provide a sensitive tool to probe multiparticle correlations [3, 4, 15, 16].

The normalised factorial moment of order q in a region of phase space of size Ω is defined as

$$F_q(\Omega) = \langle n(n-1) \cdots (n-q+1) \rangle / \langle n \rangle^q, \quad q \geq 1. \quad (1)$$

Here n is the number of particles in Ω and the angle brackets $\langle \cdots \rangle$ denote the average over events. For uncorrelated particle production within Ω one has $F_q = 1$ for all q . The factorial moments describe *many*-particle distributions via the relation $\langle n(n-1) \cdots (n-q+1) \rangle = \int_{\Omega} \rho_q(p_1, \dots, p_q) \prod_{i=1}^q dp_i$ between the unnormalised factorial moments in a region Ω and the inclusive q -particle densities, $\rho_q(p_1, \dots, p_q)$, of particles with momenta p_i .

The normalised factorial cumulants, $K_q(\Omega)$, or cumulants for short [17–19], are related

to the factorial moments $F_q(\Omega)$ through the following relations:

$$K_2 = F_2 - 1, \quad K_3 = F_3 - 3 F_2 + 2, \quad K_4 = F_4 - 4 F_3 + 3 F_2^2 + 12 F_2 - 6. \quad (2)$$

By construction, K_q is a measure of *genuine* multiparticle correlations: K_q , representing the correlation function averaged over the region Ω , vanishes whenever any one of the q particles is statistically independent of the others. For uncorrelated particle production, or Poissonian emission, within Ω one has $K_q = 0$ for $q > 1$.

The normalised factorial moments of the multiplicity distribution of gluons which are restricted in either transverse momentum $p_T < p_T^{\text{cut}}$ (cylindrically-cut phase space) or absolute momentum $p < p^{\text{cut}}$ (spherically-cut phase space) are predicted to have the following qualitative behaviour [10]:

$$F_q(p_T^{\text{cut}}) \simeq 1 + \frac{q(q-1)}{6} \frac{\ln(p_T^{\text{cut}}/Q_0)}{\ln(E/Q_0)} \quad \text{for } p_T^{\text{cut}} \rightarrow Q_0, \quad (3)$$

and

$$F_q(p^{\text{cut}}) \simeq C_1(q) > 1 \quad \text{for } p^{\text{cut}} \rightarrow 0 \text{ GeV}, \quad (4)$$

where E is the energy of the initial parton, and transverse momentum is defined with respect to its direction. Here and below the C -functions are q -dependent constants. The cumulants (2) are predicted to behave as

$$K_q(p_T^{\text{cut}}) \propto \left(\frac{\ln(p_T^{\text{cut}}/Q_0)}{\ln(E/Q_0)} \right)^{q-1} \quad \text{for } p_T^{\text{cut}} \rightarrow Q_0. \quad (5)$$

Equation (5) shows that the lower-order cumulants dominate at small p_T^{cut} . The spherically-cut cumulants are predicted to behave similarly to factorial moments, Eq. (4):

$$K_q(p^{\text{cut}}) \simeq C_2(q) > 0 \quad \text{for } p^{\text{cut}} \rightarrow 0 \text{ GeV}. \quad (6)$$

Equations (3)-(6) illustrate the different influence angular ordering has on the multiplicity moments and correlations. Cylindrically-cut moments show positive correlations but approach the Poisson limit as p_T^{cut} approaches Q_0 . On the other hand, for soft gluons with limited absolute momenta, $p < p^{\text{cut}}$, the multiplicity distribution remains broader than a Poisson distribution for any (small) value of p^{cut} .

In [10], the analytical results have been tested at parton level using the shower Monte Carlo program ARIADNE [14]. The moments $F_q(p_T^{\text{cut}})$ indeed show the expected decrease for small values of the cut, $p_T^{\text{cut}} \leq 4 \text{ GeV}$; however, they do not fully reach the Poisson value for $p_T^{\text{cut}} \rightarrow Q_0$ but saturate at values somewhat larger than one. On the other hand, $F_q(p^{\text{cut}})$ moments attain a maximum around $p^{\text{cut}} \approx 2 \text{ GeV}$, and then decrease towards finite values much above unity for $p^{\text{cut}} \rightarrow 0 \text{ GeV}$ showing that in spherically-cut phase space there is no Poisson regime.

3 Experimental details

3.1 The OPAL detector

The OPAL detector, operated from 1989 to 2000 at LEP, is described in detail elsewhere [20]. The results presented here are mainly based on the information from the tracking system, which consisted of a silicon microvertex detector, an inner vertex chamber, a jet chamber with 24 sectors each containing 159 axial anode wires, and outer z -chambers to improve the z coordinate resolution¹. The tracking system was located in a 0.435 T axial magnetic field and measured p_{\perp} , the track momentum transverse to the beam axis, with a precision of $(\sigma_{p_{\perp}}/p_{\perp}) = \sqrt{(0.02)^2 + (0.0015 p_{\perp})^2}$ (p_{\perp} in GeV) for $|\cos\theta| < 0.73$.

3.2 Data and Monte Carlo samples

This analysis is based on a data sample of approximately 3.9×10^6 hadronic Z decays collected with the OPAL detector between 1991 and 1995. About 91% of this sample was taken close to the peak of the Z; the remaining part has a centre-of-mass energy, \sqrt{s} , within ± 3 GeV of the Z peak.

Further selection criteria are based on a hadronic event selection procedure described in detail in [21]. For each event tracks were accepted only if they had at least 20 measured points in the jet chamber, the first hit closer than 70 cm to the beam axis, the measured closest distance to the e^+e^- collision point less than 5 cm in the plane perpendicular to the beam axis and less than 40 cm along the beam axis, $p_{\perp} > 0.15$ GeV, and $|\cos\theta| < 0.94$.

The event was then required to have at least five tracks, a momentum imbalance, defined as the magnitude of the vector sum of momenta of all charged particles, below $0.4\sqrt{s}$, a total energy of the tracks (assumed to be pions) greater than $0.2\sqrt{s}$, and $|\cos\theta_{\text{thr}}| < 0.9$, where θ_{thr} is the polar angle of the event thrust axis with respect to the beam direction calculated using all tracks as well as electromagnetic and hadronic calorimeter clusters. These criteria provide rejection against background from non-hadronic Z decays, two-photon and beam-wall interactions, beam-gas scattering, and ensure that the event is well contained inside the detector. A total of about 2.9 million events remain after the selection has been applied and are used for further analysis.

The kinematic variables used in the analysis are defined with respect to the event thrust axis. To remain consistent with the theoretical calculations and with similar measurements in deep-inelastic scattering, factorial moments and cumulants are calculated for all charged particles in a single event-hemisphere, defined by a plane perpendicular to the event thrust axis. The particles are assigned positive rapidity, $y = 0.5 \ln[(E + p_L)/(E - p_L)]$, with E and p_L the energy (assuming the pion mass) and longi-

¹OPAL uses the right-handed coordinate system defined with the positive z along the direction of the e^- beam and the positive x axis pointing towards the centre of the LEP ring. r is the coordinate normal to the beam axis, φ the azimuthal angle with respect to the x axis, θ the polar angle with respect to the z -axis.

tudinal momentum component of the particle, and a single randomly chosen hemisphere for each event is used in the analysis.

To correct the measured factorial and cumulant moments for the effects of detector response, initial-state radiation, resolution and particle decays, we apply the correction procedure adopted in our earlier studies [22, 23]. Two samples of more than three million multihadronic events each were used, generated with the JETSET 7.4/PYTHIA 6.2 Monte Carlo model [24]. The first sample does not include the effects of initial-state radiation, and all particles with lifetimes longer than 3×10^{-10} s were considered to be stable. The generator-level factorial moments, $F_q(\Omega)_{\text{gen}}$, are calculated directly from the charged particle multiplicity distributions of this sample without any selection criteria. The second sample was generated including the effects of finite lifetimes and initial-state radiation and was passed through a full simulation of the OPAL detector [25]. The corresponding detector-level moments, $F_q(\Omega)_{\text{det}}$, are calculated from this set using the same reconstruction and selection algorithms as used for the measured data. The corrected moments are then determined by multiplying the measured ones by the correction factors $U_q(\Omega) = F_q(\Omega)_{\text{gen}}/F_q(\Omega)_{\text{det}}$. The correction factors vary between about 0.85 and 1.2.

As systematic uncertainties, we include the following contributions:

- The statistical error on the correction factors $U_q(\Omega)$: due to the finite statistics of the Monte Carlo samples these are comparable to those of the data.
- Track and event selection criteria variations as in [22, 23]. The moments have been computed changing in turn the following selection criteria: the first measured point was required to be closer than 40 cm to the beam, the momentum was required to be less than 40 GeV, the track polar angle acceptance was changed to $|\cos \theta| < 0.7$. The changes in the corrected moments when the analysis is performed with these cuts were taken as systematic uncertainties. These changes modify the results by no more than a few percent in the smallest phase space regions and do not affect the conclusions.
- Resonance decays: We have repeated our calculations with the PYTHIA 6.2 Monte Carlo model where no decays of resonances were allowed. The difference between these calculations and those based on the sample generated including the resonance decays are taken as systematic uncertainties and do not exceed 2%.
- Two-jet selection criteria: For comparison with ZEUS data [12] where the rate of hard jet production is lower than in e^+e^- annihilation at LEP, we have calculated the moments for two-jet events selected via a thrust value cut as given in Sect. 4.3. Therefore, for the results presented in Sect. 4.3 only, we have repeated calculations for two-jet events using the Durham jet finder [26]. We apply this algorithm with the jet resolution parameter $y_{\text{cut}} = 0.03$, shown [27] to result in well separated jets while still yielding reasonable event statistics. The changes in the results based on the two selection methods are taken as systematic uncertainties. These results agree to within 7%.

- HERWIG based correction factors U_q : The correction factors $U_q(\Omega)$ were derived from samples generated with the HERWIG Monte Carlo [28]. The differences compared to PYTHIA are taken as systematic uncertainties and do not exceed 10%.

The total errors have been calculated by adding the systematic and statistical uncertainties in quadrature and are therefore correlated bin-to-bin. It was further verified that our conclusions remain unchanged when events taken at energies off the Z peak are excluded from the analysis.

The data are compared to model predictions calculated using the following Monte Carlo generators:

- PYTHIA version 6.2 [24] with the parton shower followed by string hadronisation.
- PYTHIA version 6.2, as above, but including the effect of Bose-Einstein correlations. These are simulated using the BE₃₂ algorithm [29] implemented in PYBOEI. In a previous OPAL study of higher-order cumulants [23] it was shown that this model accounts simultaneously for the magnitude and bin-size dependence of cumulants of like-sign as well as of all-charge multiplets in one- to three-dimensional phase space. Here we use a Gaussian parametrisation with PYBOEI and QCD/fragmentation parameters from [30].
- ARIADNE version 4.1 [14] with the colour dipole model for the parton shower followed by fragmentation as in JETSET/PYTHIA.
- HERWIG version 6.3 [28] with a parton shower followed by cluster fragmentation.

Each Monte Carlo sample consists of more than three million events. The simulation parameters of the JETSET/PYTHIA and HERWIG models have been tuned to OPAL data in [31]. The parameters of ARIADNE and recent changes for the HERWIG parameters² are given in [32]. The errors of the Monte Carlo predictions are comparable to those of the data.

4 Results

4.1 Factorial moments

Fig. 1 shows cylindrically cut factorial moments F_q of order $q = 2$ to 5 as a function of p_T^{cut} .³ With decreasing p_T^{cut} , the moments decrease towards a minimum at a common value of $p_T^{\text{cut}} \approx 1$ GeV but remain larger than unity, the Poisson value. The observed deviation of the p_T^{cut} -dependence from the Poissonian behaviour for large p_T^{cut} values agrees qualitatively with the theoretical expectation discussed in Sect. 2. However, for smaller

²Here we used PSPLT(1) = 0.6 and CLMAX = 3.6 GeV instead of 1.0 and 3.35 GeV.

³The numerical values of the data on factorial moments and cumulants will be made available in the Durham HEP Database, <http://durpdg.dur.ac.uk/HEPDATA>.

p_T^{cut} values the moments rise strongly, in clear disagreement with the perturbative QCD result for partons. Figure 1 suggests that the predicted Poisson limit for soft gluons is masked by strong hadronisation effects as $p_T^{\text{cut}} \rightarrow Q_0$. The drop of the moments and the characteristic dip for $p_T^{\text{cut}} \simeq 1$ GeV indicate, however, that perturbative calculations may be relevant for hadrons down to a scale of approximately 1 GeV.

The Monte Carlo model calculations which include both the parton cascade and hadronisation, largely follow the trend of the data and, in particular, reproduce the minimum around $p_T^{\text{cut}} = 1$ GeV. Differences appear for $p_T^{\text{cut}} \lesssim 1$ GeV, with HERWIG describing the data better than the models using string fragmentation. However, the dotted curves, which represent PYTHIA predictions with the inclusion of Bose-Einstein correlations, are in very good agreement with the measurements.

To study the influence of resonance decays, event samples were generated wherein resonances were not allowed to decay. The enhancement for $p_T^{\text{cut}} \lesssim 1$ GeV remained almost unaffected in the case of the PYTHIA model. For the HERWIG model, the suppression of the decays led to an increase of the factorial moments below $p_T^{\text{cut}} \approx 0.5$ GeV, an effect also observed in e^+p studies [12]. This increase ranges from a few percent for $q = 2$ to about 20% for $q = 5$.

Fig. 2 shows spherically cut factorial moments F_q , $q = 2$ to 5, as a function of p^{cut} . For large p^{cut} values the moments change very little owing to the kinematically limited number of particles per event at high momenta. However, for smaller p^{cut} the moments increase rapidly and show no tendency to level off for $p^{\text{cut}} \rightarrow 0$ GeV, contrary to theoretical predictions for partons. The Monte Carlo models describe the data rather well down to $p^{\text{cut}} \simeq 2-3$ GeV. In that region they are, in fact, very similar to parton-level (and hadron-level) predictions from ARIADNE shown in [10]. For smaller values, and in sharp contrast to the data, the Monte Carlo curves flatten off and remain approximately constant, a feature also observed in [10]. The influence of Bose-Einstein correlations, as implemented in PYTHIA, is sizeable in that region but insufficient to reproduce the data. Indeed, the LEP measurements [33] have shown that BEC effect is expected to be larger in the longitudinal direction than that in the transverse direction of the jet, though this is not implemented in PYTHIA.

4.2 Factorial cumulants

The large statistics available in this analysis allows the study of the factorial cumulants, $K_q(p_T^{\text{cut}})$ and $K_q(p^{\text{cut}})$, defined in (2). These are a direct measure of the genuine correlations among hadrons and thus present the information in a way which can more readily be interpreted. Fig. 3 shows the cylindrically cut and spherically cut cumulants of order $q = 3, 4$.⁴

The cumulant $K_3(p_T^{\text{cut}})$ has a similar p_T^{cut} -dependence to the factorial moments: it is positive at large p_T^{cut} , decreases towards a minimum, close to zero around $0.6 - 0.7$ GeV and rises rapidly as p_T^{cut} is further decreased. Interestingly, the minimum occurs at a

⁴Note that K_2 is, by definition, equal to $F_2 - 1$ and therefore not shown here.

smaller p_T^{cut} value than that for $K_2(p_T^{\text{cut}})$ (or $F_2 - 1$, Fig. 1) and for the higher-order factorial moments. Four-particle correlations, measured by $K_4(p_T^{\text{cut}})$, are compatible with zero, within errors. From the rapid increase of $K_2(p_T^{\text{cut}})$ and $K_3(p_T^{\text{cut}})$ as $p_T^{\text{cut}} \rightarrow 0$ GeV, we can conclude that the strong rise of the factorial moments is predominantly due to genuine particle correlations.

Figure 3 shows that the cumulants in spherically cut phase space are significantly larger than the $K_q(p_T^{\text{cut}})$ cumulants for p^{cut} smaller than a few GeV. They continue to increase with decreasing p^{cut} , a behaviour reflected in the corresponding factorial moments in Fig. 2.

The various Monte Carlo models, shown in Fig. 3, agree qualitatively with the measurements but differ in detail for all p_T^{cut} and $p^{\text{cut}} < 2$ GeV values. The largest deviations occur for the cumulants $K_q(p^{\text{cut}})$ below $p^{\text{cut}} \simeq 2$ GeV where the models start to level off, whereas the measured cumulants continue to increase as $p^{\text{cut}} \rightarrow 0$ GeV. Suppression of resonance decays in HERWIG was found to increase the cumulants $K_q(p_T^{\text{cut}})$ for p_T^{cut} below 1 GeV. In contrast, the spherically-cut cumulants predicted by HERWIG remain essentially unchanged.

The results presented above might potentially be biased due to correlations induced by Dalitz decays ($\pi^0 \rightarrow \gamma e^+ e^-$) and fake pairs. The former would manifest themselves as a narrow peak in the invariant mass distribution of unlike-sign particle pairs near threshold. No such enhancement was found in the data. The check against fake pairs showed a peak at very small invariant masses which was found not to influence the results.

We have also repeated the analysis for multiplets composed of like-sign particles. Although the corresponding moments differ in magnitude, their dependence on p_T^{cut} and p^{cut} (not shown) follows closely that of all-charge particle moments. We may therefore conclude that the dip-structure observed in Fig. 1 and Fig. 3 is stable against changes in the charge composition of the multiplets.

4.3 Comparison with deep-inelastic scattering

The ZEUS measurements reported in [12] were carried out in the current region of the Breit frame of reference which is traditionally considered to be the equivalent of a single event-hemisphere in e^+e^- annihilation [13]. A sample of e^+p interactions was used with an average four-momentum transfer squared of $\langle Q^2 \rangle \simeq 2070$ GeV². This corresponds to an equivalent e^+e^- c.m.s. energy, \sqrt{s} , of 44 GeV.

The factorial moments studied in [12] show many of the characteristics also reported here. However, an interesting difference is observed in the p_T^{cut} dependence of the factorial moments. The distinctive minimum seen in the OPAL data for $p_T^{\text{cut}} \approx 1$ GeV, which could signal the borderline between perturbative and non-perturbative dynamics, is absent in the ZEUS measurements. The latter remain constant down to $p_T^{\text{cut}} = 1$ GeV below which value they increase rapidly. The authors interpret their measurements as the first indication that perturbative QCD fails on a qualitative level to describe the hadronic multiplicities and that hadronisation causes a violation of the LPHD hypothesis for many-particle inclusive observables.

To try and understand the differences between the e^+e^- and e^+p results, we have carried out further studies to mimic the ZEUS experimental conditions. These differ significantly from those in e^+e^- annihilation: (i) the selected current region of the Breit frame excludes a large part of the central rapidity region in the γ^* -proton rest-frame, the equivalent of the c.m.s frame in e^+e^- , which is included in our analysis; (ii) the rate of hard jet production is lower in e^+p collisions at HERA energies than in e^+e^- at LEP.

To study the influence of the central rapidity region and the hard jet production rate, we have repeated the analysis for rapidity intervals $y > y_0$ with $y_0 \geq 1$ and for two-jet events, the latter selected through a cut on the thrust value.

As an example, Fig. 4 shows the moments $F_q(p_T^{\text{cut}})$ for $y_0 = 1.5$. Omitting the central region in the OPAL data clearly has a strong effect on the magnitude and p_T^{cut} -dependence of the moments. In particular, the minimum around $p_T^{\text{cut}} = 1$ GeV, seen in the full sample ($y > 0$) is absent when only hadrons with $y > 1.5$ are selected. The ZEUS and OPAL data ($y > 1.5$) overlap for $q = 2$ in the full p_T^{cut} region; higher order moments are very similar below p_T^{cut} of about 1 GeV but differ in magnitude at higher p_T^{cut} .

In Figure 4 we also show results for two-jet events. These events were selected by requiring the thrust value of an event to be larger than 0.96. The sample corresponds to about 30% of all multi-hadronic events. An alternative two-jet selection based on the Durham jet-finder [26] led to very small differences which are included in the systematic uncertainties.

Selecting two-jet events reduces significantly the values of the factorial moments (and cumulants, not shown) for all p_T^{cut} in comparison with those in the inclusive sample. The OPAL measurements are lower than the ZEUS data but, as expected, show qualitatively the same behaviour: constant down to $p_T^{\text{cut}} \approx 1$ GeV followed by a strong rise as $p_T^{\text{cut}} \rightarrow 0$ GeV, with no evidence for a distinct minimum near 1 GeV.

The OPAL results on rapidity-restricted factorial moments suggest that the often assumed equivalence of a single event-hemisphere in e^+e^- annihilation with the current region in the Breit frame for deep-inelastic e^+p interactions has to be treated with caution. In theoretical predictions for QCD cascades, which apply to the whole jet and moreover focus on soft gluon emissions, characteristic signatures of soft particle emission, such as colour coherence, are seen only if particles with small rapidities are also included. Likewise, selecting two-jet events may introduce a bias which can mask the effect under study. Our findings suggest an explanation for the differences obtained in the ZEUS analysis [9] of angular correlations compared to the LEP results [8].

5 Summary and conclusions

Analytical perturbative QCD calculations, in agreement with parton-level Monte Carlo calculations, show that gluons produced in a jet become uncorrelated when the gluon transverse momentum relative to the jet axis, p_T , is restricted to small values. The approach to a Poisson regime is a direct consequence of colour coherence, or angular ordering of gluon emissions in the QCD cascade and is expected to hold also for soft

hadrons if Local Parton-Hadron Duality (LPHD) is valid.

In this paper, the predicted QCD colour coherence effect has been tested in e^+e^- annihilation at the Z-resonance using factorial moments and factorial cumulants of the multiplicity distribution of hadrons with restricted transverse momenta $p_T < p_T^{\text{cut}}$ or restricted absolute momenta $p \equiv |\mathbf{p}| < p^{\text{cut}}$. The analysis is based on a data sample of about four million events recorded with the OPAL detector at LEP.

For cylindrically cut phase space, the factorial and cumulant moments are predicted by analytical QCD calculations to reach limiting values close to unity and zero, respectively, for small p_T^{cut} . Likewise, in spherically cut phase space, the factorial and cumulant moments should saturate at values well above unity and zero, respectively, for $p^{\text{cut}} \rightarrow 0$ GeV. These expectations are not borne out by the measurements: for $p_T^{\text{cut}} \lesssim 1$ GeV or for values of p^{cut} below a few GeV, the moments and cumulants rise strongly with decreasing p_T^{cut} or p^{cut} . QCD based Monte Carlo models which include hadronisation, reproduce well the change in correlation pattern but serious discrepancies remain in the very low momentum region. However, Bose-Einstein correlations, as implemented in PYTHIA, significantly improve the agreement between data and Monte Carlo predictions.

Interestingly, in the region of large to intermediate p_T^{cut} , a minimum around 1 GeV is observed in the p_T^{cut} dependence of the factorial moments, with a corresponding minimum, close to zero, at $p_T^{\text{cut}} \simeq 0.6$ GeV for the cumulant K_3 , as expected from colour coherence. One may interpret the intermediate p_T^{cut} -range 0.6 – 1.0 GeV as a borderline between a regime of perturbative dynamics where the LPHD hypothesis is justified, and a regime dominated by strong confinement forces which leads to violation of LPHD for many-particle inclusive observables.

In a similar analysis in deep inelastic e^+p scattering at HERA, no evidence was found for a Poisson-like regime in cylindrically-cut phase space. The results presented here show that the characteristic decrease towards a minimum around p_T^{cut} of 1 GeV disappears if hadrons produced in the central region of rapidity ($y \lesssim 1$) are excluded, or if the analysis is restricted to two-jet events. The former suggests that, for soft particle production, the often assumed equivalence of a single event-hemisphere in e^+e^- annihilation with the current region in the Breit frame of a deep inelastic e^+p collision may be misleading.

Acknowledgements

We thank Wolfgang Ochs for helpful discussions. We particularly wish to thank the SL Division for the efficient operation of the LEP accelerator at all energies and for their close cooperation with our experimental group. In addition to the support staff at our own institutions we are pleased to acknowledge the
 Department of Energy, USA,
 National Science Foundation, USA,
 Particle Physics and Astronomy Research Council, UK,
 Natural Sciences and Engineering Research Council, Canada,
 Israel Science Foundation, administered by the Israel Academy of Science and Humani-

ties,

Benozio Center for High Energy Physics,

Japanese Ministry of Education, Culture, Sports, Science and Technology (MEXT) and
a grant under the MEXT International Science Research Program,

Japanese Society for the Promotion of Science (JSPS),

German Israeli Bi-national Science Foundation (GIF),

Bundesministerium für Bildung und Forschung, Germany,

National Research Council of Canada,

Hungarian Foundation for Scientific Research, OTKA T-038240, and T-042864,

The NWO/NATO Fund for Scientific Research, the Netherlands.

References

- [1] B.I. Ermolayev, V.S. Fadin, JETP Lett. **33** (1981) 285;
A.H. Mueller, Phys. Lett. B **104** (1981) 161.
- [2] Yu.L. Dokshitzer *et al.*, *Basics of Perturbative QCD* (Editions Frontières, Gif-sur-Yvette, 1991).
- [3] V.A. Khoze, W. Ochs, Int. J. Mod. Phys. A **12** (1997) 2949;
V.A. Khoze, W. Ochs, J. Wosiek, in: *At the Frontier of Particle Physics: Handbook of QCD* (Ed. M.A. Shifman), Vol. 2 (World Scientific Co., 2001), p. 1101.
- [4] I.M. Dremin, J.W. Gary, Phys. Reports **349** (2001) 301;
I.M. Dremin, Physics - Uspekhi **45** (2002) 507.
- [5] G. Dissertori, I. Knowles, M. Schmelling, *Quantum Chromodynamics: High Energy Experiments and Theory* (Oxford University Press, Oxford, 2003).
- [6] Ya.I. Azimov *et al.*, Sov. J. Nucl. Phys. **40** (1984) 817, Z. Phys. C **27** (1985) 65, Z. Phys. C **31** (1986) 213;
D. Amati, G. Veneziano, Phys. Lett. B **83** (1979) 87;
G. Marchesini, L. Trentadue, G. Veneziano, Nucl. Phys. B **181** (1981) 335.
- [7] ZEUS Collaboration, J. Breitweg *et al.*, Eur. Phys. J. C **11** (1999) 251.
- [8] L3 Collaboration, M. Acciarri *et al.*, Phys. Lett. B **428** (1998) 186;
DELPHI Collaboration, M. Abreu *et al.*, Phys. Lett. B **440** (1998) 203;
DELPHI Collaboration, M. Abreu *et al.*, Phys. Lett. B **457** (1999) 368.
- [9] ZEUS Collaboration, J. Breitweg *et al.*, Eur. Phys. J. C **12** (2000) 53.
- [10] S. Lupia, W. Ochs, J. Wosiek, Nucl. Phys. B **540** (1999) 405.
- [11] Z. Koba, H.B. Nielsen, P. Olesen, Nucl. Phys. B **40** (1972) 317.
- [12] ZEUS Collaboration, S. Chekanov *et al.*, Phys. Lett. B **510** (2001) 36.
- [13] R.P. Feynman, *Photon-Hadron Interactions* (Benjamin, New York, 1972).
- [14] L. Lönnblad, Comp. Phys. Comm. **71** (1992) 15.
- [15] E.A. De Wolf, I.M. Dremin, W. Kittel, Phys. Reports **270** (1996) 1.
- [16] W. Kittel, E.A. De Wolf, *Soft Multihadron Dynamics* (World Scientific, Singapore, 2005).
- [17] A.H. Mueller, Phys. Rev. D **4** (1971) 150.
- [18] P. Carruthers, I. Sarcevic, Phys. Rev. Lett **63** (1989) 1562.

- [19] E.A. De Wolf, *Acta Phys. Pol. B* **21** (1990) 611.
- [20] OPAL Collaboration, K. Ahmet *et al.*, *Nucl. Instr. Meth. A* **305** (1991) 275;
P.P. Allport *et al.*, *Nucl. Instr. Meth. A* **346** (1994) 476.
- [21] OPAL Collaboration, G. Alexander *et al.*, *Z. Phys. C* **52** (1991) 175.
- [22] OPAL Collaboration, G. Abbiendi *et al.*, *Eur. Phys. J. C* **11** (1999) 239.
- [23] OPAL Collaboration, G. Abbiendi *et al.*, *Phys. Lett. B* **523** (2001) 35.
- [24] T. Sjöstrand, *Comp. Phys. Comm.* **82** (1994) 74;
T. Sjöstrand *et al.*, *Comp. Phys. Comm.* **135** (2001) 238;
T. Sjöstrand, L. Lönnblad, S. Mrenna, LU TP 01-21 (2001), hep-ph/0108264.
- [25] J. Allison *et al.*, *Nucl. Instr. Meth. A* **317** (1992) 47.
- [26] S. Catani *et al.*, *Phys. Lett. B* **269** (1991) 432.
- [27] OPAL Collaboration, R. Akers *et al.*, *Z. Phys. C* **65** (1995) 367;
JADE Collaboration, P. Pfeifenschneider *et al.*, OPAL Collaboration, G. Abbiendi *et al.*, *Eur. Phys. J. C* **17** (2000) 19.
- [28] G. Corcella *et al.*, *JHEP* **0101** (2001) 010.
- [29] L. Lönnblad, T. Sjöstrand, *Eur. Phys. J. C* **2** (1998) 165.
- [30] OPAL Collaboration, G. Abbiendi *et al.*, *Eur. Phys. J. C* **36** (2004) 297.
- [31] OPAL Collaboration, G. Alexander *et al.*, *Z. Phys. C* **69** (1996) 543.
- [32] OPAL Collaboration, G. Abbiendi *et al.*, *Eur. Phys. J. C* **35** (2004) 293.
- [33] L3 Collaboration, M. Acciarri *et al.*, *Phys. Lett. B* **458** (1999) 517;
DELPHI Collaboration, P. Abreu *et al.*, *Phys. Lett. B* **471** (2000) 460;
OPAL Collaboration, G. Abbiendi *et al.*, *Eur. Phys. J. C* **16** (2000) 423;
ALEPH Collaboration, A. Heister *et al.*, *Eur. Phys. J. C* **36** (2004) 147.

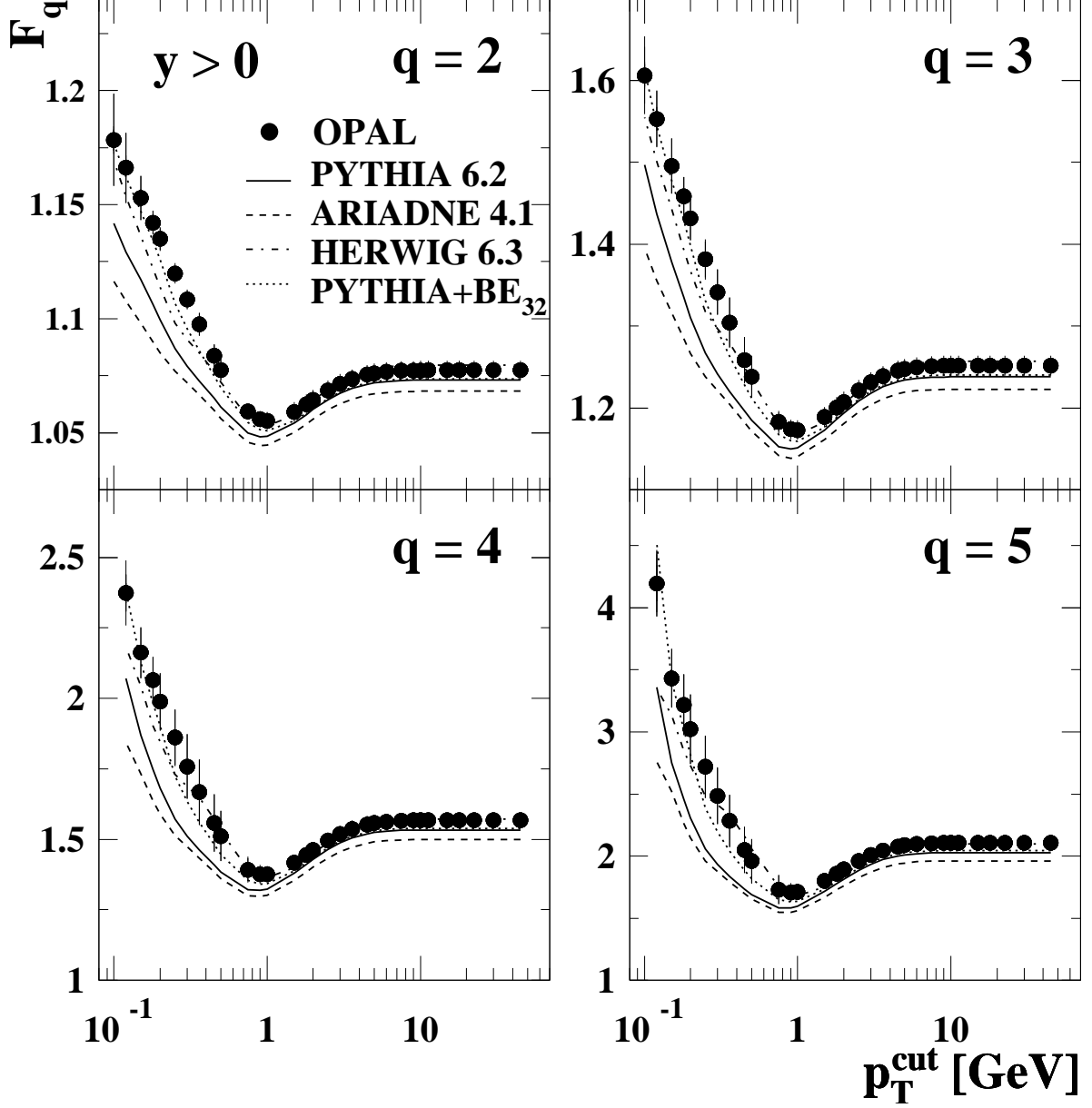


Figure 1: Factorial moments of charged particles with transverse momenta $p_T < p_T^{\text{cut}}$ as a function of p_T^{cut} compared to different Monte Carlo predictions. The error bars, shown where larger than the marker size, represent the statistical and systematic uncertainties added in quadrature. The dotted line shows Monte Carlo predictions from PYTHIA with Bose-Einstein correlations included (see text). The errors of the Monte Carlo predictions are comparable to those of the data.

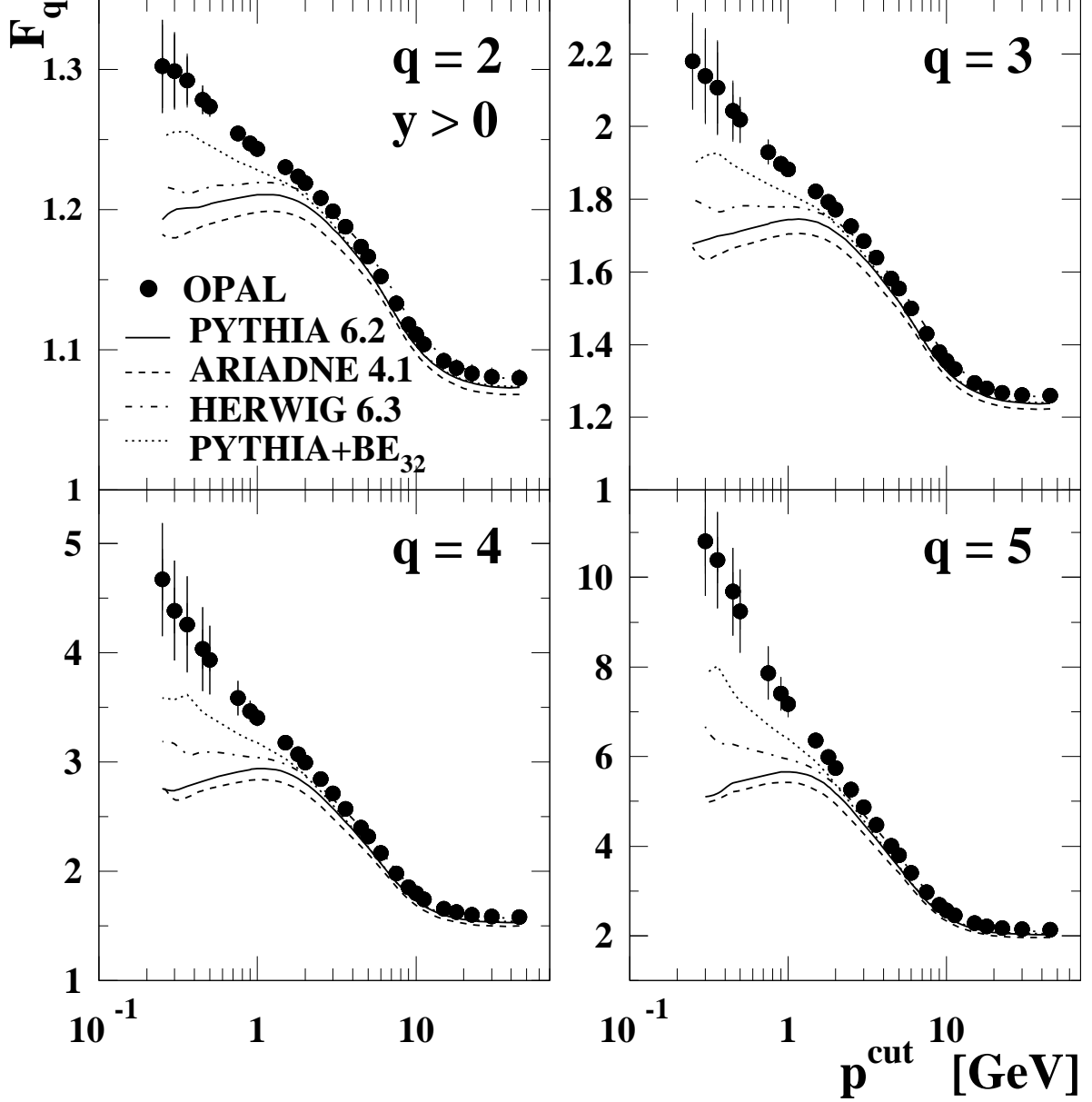


Figure 2: Factorial moments of charged particles with absolute momenta $p \equiv |\mathbf{p}| < p^{\text{cut}}$ as a function of the momentum cut, p^{cut} compared to different Monte Carlo predictions. The error bars, shown where larger than the marker size, represent the statistical and systematic uncertainties added in quadrature. The dotted line shows Monte Carlo predictions from PYTHIA with Bose-Einstein correlations included (see text). The errors of the Monte Carlo predictions are comparable to those of the data.

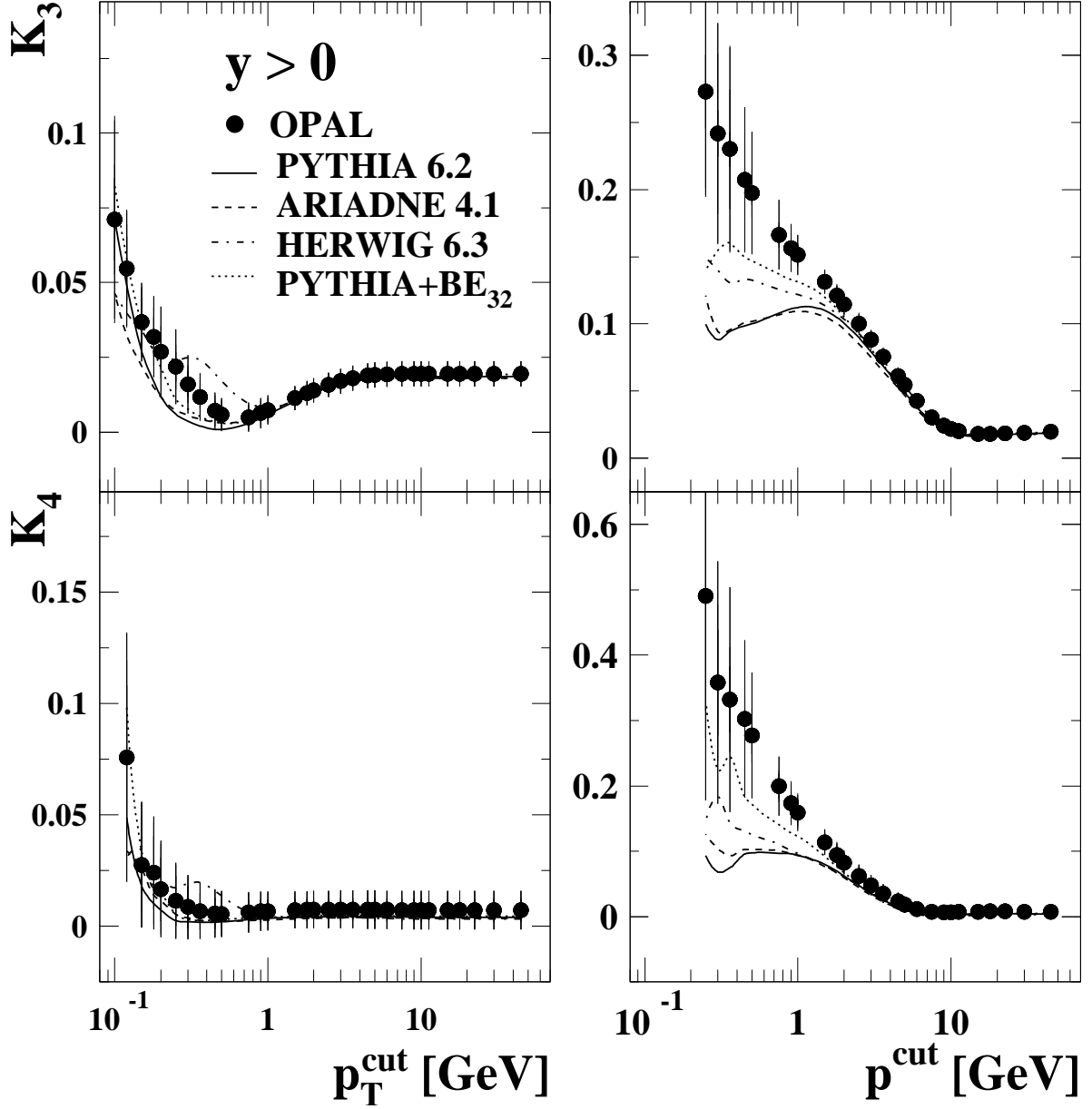


Figure 3: K_3 and K_4 cumulants of charged particles with transverse momenta $p_T < p_T^{\text{cut}}$ as a function of the momentum cut p_T^{cut} (left panel) and with absolute momenta $p < p^{\text{cut}}$ as a function of the momentum cut p^{cut} (right panel) compared to different Monte Carlo predictions. The error bars, shown where larger than the marker size, represent the statistical and systematic uncertainties added in quadrature. The errors are correlated bin-to-bin. The dotted line shows Monte Carlo predictions from PYTHIA with Bose-Einstein correlations included (see text). The errors of the Monte Carlo predictions are comparable to those of the data.

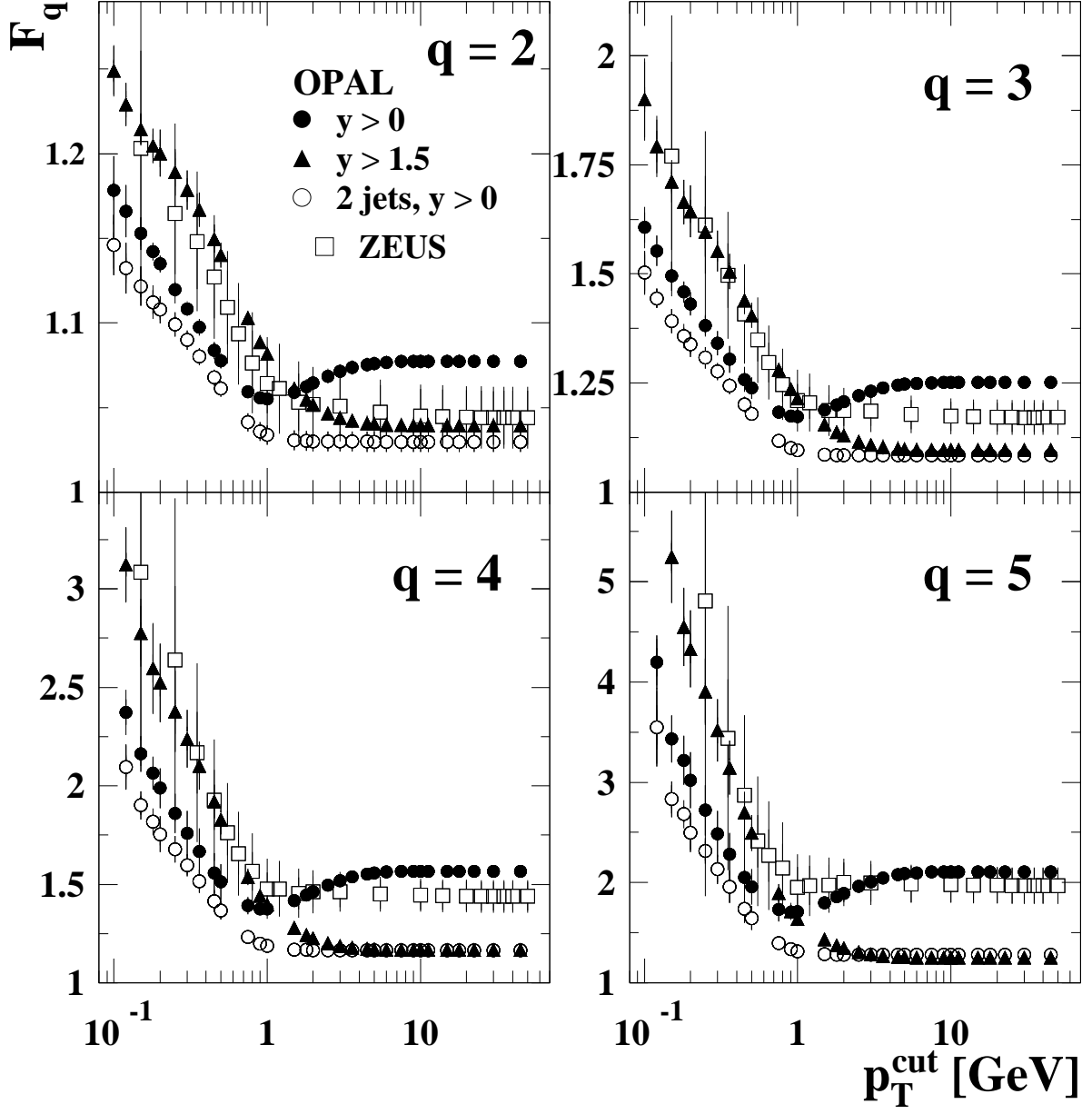


Figure 4: Factorial moments of charged particles with absolute momenta $p_T < p_T^{\text{cut}}$ as a function of p_T^{cut} , compared to those of 2-jet events, in the rapidity window $y > 1.5$ and data from ZEUS [12]. The error bars, shown where larger than the marker size, represent the statistical and systematic uncertainties added in quadrature.